Single-Phase Rectifier with High Power Factor and Low-Frequency Switching

Eduardo da Silva Martins, Giorgio Spiazzi* and José Antenor Pomilio

School of Electrical and Computer Engineering, University of Campinas
C. P. 6101 13081-970 Campinas – BRAZIL
Tel. (+55-19) 7883748 – Fax (+55-19) 2891395
e-mail: antenor@dsce.fee.unicamp.br

**Department of Electronics and Informatics, University of Padova*
Via Gradenigo 6A - 35131 Padova - ITALY
Tel. (+39-049) 827-7525 - Fax (+39-049) 827-7699
e-mail: spiazzi@dei.unipd.it

Abstract. **The paper presents a simple cell with a line-frequency commutated AC switch that is able to greatly improve both power factor and output voltage regulation of rectifiers with passive L-C filters. The boost action introduced by the commutation cell allows for the compensation of the voltage drop across the input filter inductor, so as output voltages higher than the peak of the line voltage can be achieved. Moreover, as compared to the line-frequency commutated boost rectifier, the proposed circuit allows compliance with the low-frequency harmonic standard EN 61000-3-2 with a lower filter inductance value, at output power levels greater than 1kW. A converter prototype was built and tested. Results are reported in order to confirm the theoretical analysis.**

I. INTRODUCTION

High frequency power factor correctors (PFCs) providing very high power factors as well as good output voltage regulation are increasingly substituting conventional front-end rectifiers due to harmonic limits imposed by international standards like IEC-61000-3-2 [1]. The penalty of such improvement in the absorbed line current is an increase of the overall ac-to-dc converter size and cost, sometimes not possible in large volume applications like household appliances, TV sets etc. In such cases, standard low-cost high-reliable rectifiers with passive filters are still used in order to improve the quality of the current drawn from the line, even if the volume of the reactive components needed becomes rapidly prohibitive as the power increases [2].

Several line frequency commutated rectifier topologies have been presented in literature as a trade-off between cost and performances [3-6]. All of them provide compliance with the standards with a lower reactive component volume, as compared with passive L-C filters. This is possible by increasing the input current conduction angle through the use of a line-frequency commutated switch, plus other few components.

The same principle is exploited in the proposed line-frequency commutation cell, which has the following advantages:

- possibility to be used in existing rectifiers with passive L-C filters;
- high power factor as compared to standard L-C rectifiers;
- inherent switch short circuit protection;
- possibility to achieve output voltage regulation in wide line and load variation ranges;
- lower inductor value needed to comply with IEC 61000-3-2 standard as compared to the line-frequency commutated boost rectifier [3,4].

As disadvantages it has the necessity of a bi-directional voltage and current switch and the switch gate drive signal must be insulated.

The operation principles of the proposed rectifier are explained in the paper and two different design procedures are suggested.

Measurements made on a converter prototype show a good agreement with the theoretical expectations.

II. PRINCIPLE OF OPERATION

A single-phase rectifier with passive L-C_L filter is shown in Fig. 1 together with the proposed line-frequency commutation cell composed by AC switch, S, and capacitors C_1 and C_2. The cell operation is described in the following with the help of Fig. 2, which reports input current, i_g, and voltage, u_2, waveforms in the first line half period, in which voltage, u_g, is positive, together with the switch gate drive signal. As we can see, two different situations can occur, depending on the capacitor initial voltage, U_{20}, as illustrated in Figs. 2a), where $U_{20} = 0$ and 2b), where $U_{20} \neq 0$. Expressions for the input current and resonant capacitor voltage are reported in Table I in normalized form by using the following base quantities and definitions:

Line voltage: ..... $u_g(\theta) = U_{pk}\sin(\theta), \theta = \omega_i t$

Base voltage: ..... $U_N = U_{pk}$ (1.a)

Base current: ..... $I_N = \dfrac{U_{pk}}{\omega_i L}$ (1.b)

Resonant angular frequency: ..... $\omega_o = \dfrac{1}{\sqrt{2LC}}$ (1.c)

Normalized resonance frequency: .. $\alpha = \dfrac{\omega_o}{\omega_i}$ (1.d)

Voltage conversion ratio: ..... $M = \dfrac{U_o}{U_{pk}}$ (1.e)

For the analysis, the output voltage ripple was neglected, so that U_o is considered constant.

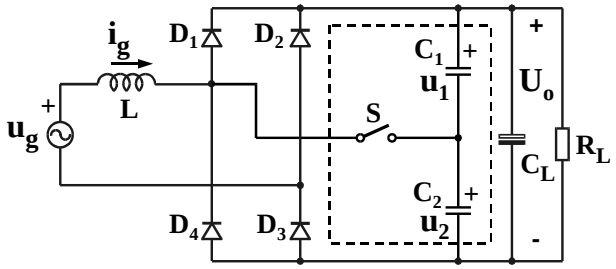

Fig.1 – Scheme of a rectifier with passive L-C_L filter with the proposed line-frequency commutation cell (S is an AC switch)

A) Resonant interval $\theta_1 < \theta \leq \theta_2$.

The switch S turns-on with a delay θ_d to the line voltage zero crossing. If the initial capacitor voltage is zero or, anyway, lower than the input voltage at this instant, the resonance cycle between the input inductor, L, and the equivalent capacitor $C_1+C_2 = 2C$ ($C_1 = C_2 = C$) starts. This is the case considered in Figs. 2a) and b). The initial angle θ_1 in which the input current starts to flow coincides with θ_d. On the other hand, if at θ_d the input voltage is lower than the initial capacitor voltage, then the input current starts to flow only when diode D_3 becomes forward biased, so that $\theta_1>\theta_d$. In summary, we can write:

$$\theta_1 = \max\left\{\theta_d, sin^{-1}\left(U_{20N}\right)\right\}, \text{ where } U_{20N} = \frac{U_{20}}{U_N} \qquad (2)$$

During the resonant interval, the input current divides almost equally ($C_L >> C_1,C_2$) between C_1 and C_2 and returns through diode D_3.

The equations describing normalized input current and capacitor voltage are reported in Table I.

This interval ends either by the switch turning-off (if U_{20} is greater than zero as shown in Fig. 2b) or by turning-on the diode D_1 (if U_{20} is zero as shown in Fig. 2a), which occurs when voltage u_2 becomes equal to the output voltage U_o.

In the first case, the final voltage on capacitor C_2, at steady state, must be equal to U_o-U_{20}. This condition can be exploited in order to calculate the initial capacitor voltage by using the equation in the last row of Table I. Such equation can be solved directly only in the case $\theta_1=\theta_d$ since the conduction angle θ_c coincides with the switch on-time, and is therefore imposed by the control (it is a known quantity in the formula).

In the other case, the equation must be solved numerically since θ_c becomes a function of U_{20}.

The case in which the input current zeroes after a half resonant cycle is not considered since it produces a high input current distortion, and must be avoided by a proper design.

B) Discharging interval $\theta_2 < \theta < \theta_3$.

At the end of the previous interval, the capacitor voltage u_2 is either U_o or U_o-U_{20} and the inductor discharges to the output filter capacitor and to the load through diodes D_1 and D_3. The equation describing the current behavior is reported in Table I. I_{g0} is the inductor current value at the end of the resonant interval. When the current goes to zero, the diodes turn-off and the energy to the load is supplied only by the output capacitor.

During the input voltage negative half cycle, the operations remain the same with a negative input current and with voltage u_1 considered instead of u_2.

As we can see, in the case ($U_{20} = 0$) the resonant interval θ_c depends only on the resonant circuit parameters L and C and on the delay angle θ_d. In the other cases it depends also on the switch on interval θ_{on}. Anyway, like other line-frequency commutated rectifiers, the resonance phase causes a strong boost action, which can easily compensate for the inductor voltage drop. Moreover, the normalized resonance frequency, α, gives another degree of freedom in the converter design, as compared to the low-frequency commutation boost rectifier [3,4], that helps to obtain a satisfactory (in terms of harmonic content) input current waveform, with a reduced inductance.

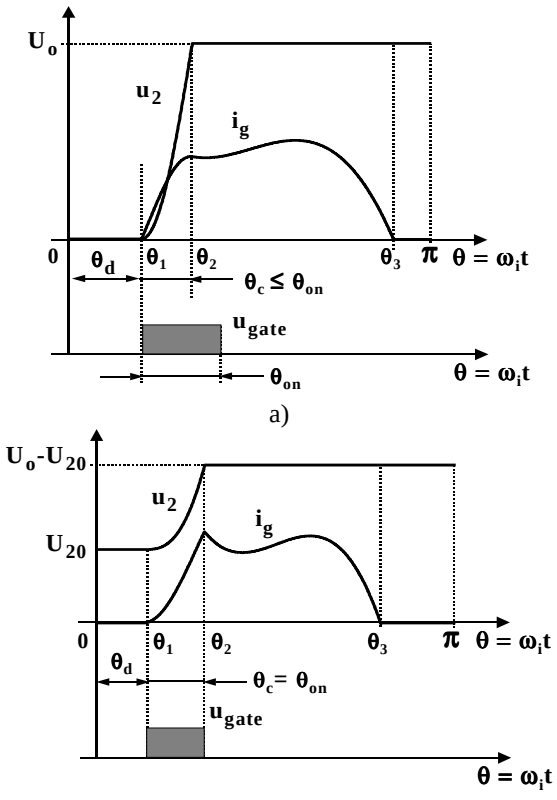

Fig.2 – Input current i_g and capacitor voltage u_2 in the first line half period. a) Initial capacitor voltage $U_{20} = 0$; b) initial capacitor voltage $U_{20} > 0$ and $U_{pk} \sin(\theta_d) > U_{20}$ ($\theta_1 = \theta_d$)

III. Design Examples

Similarly to other line-frequency commutated rectifiers, there are many parameters (inductance value, resonance frequency, delay and turn-on times) that influence, in a complex way, the input current waveform and the output voltage and power. Thus, different design approaches can be developed, depending on the desired goal. In the following, two different design examples are presented in order to show the converter potentiality.

TABLE I - EQUATIONS DESCRIBING NORMALIZED INPUT CURRENT I_{gN} AND CAPACITOR VOLTAGE U_{2N} IN A LINE HALF PERIOD

Intervals	Fundamental equations
$0 \le \theta \le \theta_1$	$i_{gN}(\theta)=0$, $u_{2N}(\theta)=U_{20N}$
$\theta_1 \le \theta \le \theta_2$	$i_{gN}(\theta)=\frac{\cos(\theta_1)}{\alpha^2-1}\{\cos(\theta-\theta_1)-\cos[\alpha(\theta-\theta_1)]\}-\frac{sin(\theta_1)}{\alpha^2-1}\{sin(\theta-\theta_1)-\alpha sin[\alpha(\theta-\theta_1)]\}-\frac{U_{20N}}{\alpha}sin[\alpha(\theta-\theta_1)]$ $u_{2N}(\theta)=U_{20N}\cos[\alpha(\theta-\theta_1)]+\frac{\alpha^2}{\alpha^2-1}\left\{\cos(\theta_1)\left\{sin(\theta-\theta_1)-\frac{1}{\alpha}sin[\alpha(\theta-\theta_1)]\right\}+sin(\theta_1)\{\cos(\theta-\theta_1)-\cos[\alpha(\theta-\theta_1)]\}\right\}$ $I_{g0N}=i_{gN}(\theta_2)$
$\theta_2 \le \theta \le \theta_3$	$i_{gN}(\theta)=I_{g0N}+\cos(\theta_2)-\cos(\theta)-M(\theta-\theta_2)$ $u_{2N}(\theta)=M-U_{20N}$
$\theta_3 \le \theta \le \pi$	$i_{gN}(\theta)=0$, $u_{2N}(\theta)=M-U_{20N}$
$U_{20N}=\frac{1}{1+\cos(\alpha\theta_c)}\left\{M-\frac{\alpha^2}{\alpha^2-1}\left[\cos(\theta_1)\left[\sin(\theta_c)-\frac{1}{\alpha}\sin(\alpha\theta_c)\right]+\sin(\theta_1)[\cos(\theta_c)-\cos(\alpha\theta_c)]\right]\right\}$	

A) Design for Maximum Voltage Regulation Range

In this design example, the goal is to maintain a constant output voltage irrespective of line and load variations. In order to do that, the input inductor and the resonant capacitor values are calculated so as to ensure a non zero input current in the whole line period at the minimum input voltage and for the desired output voltage and power, assuming the switch is always kept on. Then, compliance with EN 61000-3-2 standard is tested at U_g = 230 V_{RMS}, as required by the norm: if it fails, a lower output voltage or a reduced input voltage range must be used. By letting $\theta_1 = \theta_d = 0$ and $U_{20} = 0$, the input current i_g and capacitor voltage u_2 equations reduce to:

$$i_{gN}(\theta)=\frac{1}{\alpha^2-1}[\cos(\theta)-\cos(\alpha\theta)] \quad (3)$$

$$u_{2N}(\theta)=\frac{\alpha^2}{\alpha^2-1}\left[sin(\theta)-\frac{1}{\alpha}sin(\alpha\theta)\right] \quad (4)$$

The conduction angle θ_c is determined by the instant in which u_2 reaches the output voltage value, i.e. from (4):

$$u_{2N}(\theta_c)=M_{\max}=\frac{\alpha^2}{\alpha^2-1}\left[sin(\theta_c)-\frac{1}{\alpha}sin(\alpha\theta_c)\right] \quad (5)$$

where the maximum desired voltage conversion ratio $M_{max} = U_o/U_{pkmin}$ is used. Then, the input current evolves as prescribed by the corresponding equation in Table I, where, in this case, $\theta_2 = \theta_c$. From this equation, by imposing $\theta_3 = \pi$, the following constraint can be derived (I_{g0N} is derived by letting $\theta = \theta_c$ in (3)):

$$\frac{1}{\alpha^2-1}\left[\alpha^2\cos(\theta_c)-\cos(\alpha\theta_c)\right]+1-M_{\max}(\pi-\theta_c)=0 \quad (6)$$

Eqs. (5) and (6) can be solved together (in a numerical way) in order to find α and θ_c. Then, from the input current waveform, the input power is calculated as follows:

$$P_{in}=\frac{1}{\pi}\int_0^{\pi}u_g(\theta)i_g(\theta)\,d\theta=$$
$$=\frac{U_{pk}^2}{\omega_i L}\frac{1}{\pi}\int_0^{\pi}u_{gN}(\theta)i_{gN}(\theta)\,d\theta=\frac{U_{pk}^2}{\omega_i L}P_{inN} \quad (7)$$

P_{inN} is the normalized input power, and the inductance value is calculated from (7) based on the desired input power. Finally, from the definition of the normalized resonance frequency α, the value of capacitor C_1 and C_2 is calculated. Fig. 3 reports the normalized input power P_{inN} and resonance frequency α, as a function of the voltage conversion ratio M, which can be used in the outlined design procedure.

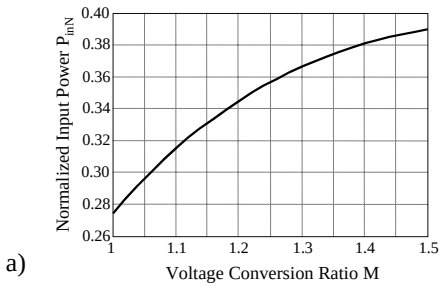

a)

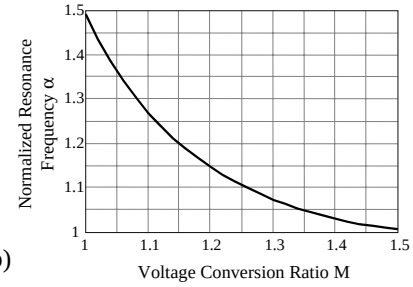

b)

Fig. 3 – Normalized input Power P_{inN} (a) and resonance frequency α (b) as a function of the voltage conversion ratio M in the case of a non zero input current in the whole line period ($\theta_3 = \pi$).

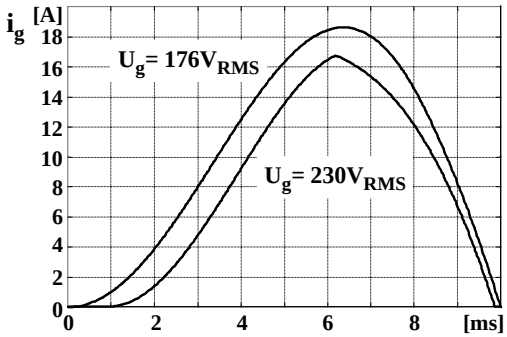

Fig. 4 – Input current waveform at two different input voltage values (P_{in} = 2kW, U_o = 350 V).

As an example, let us consider the following specifications:

Input voltage: U_g = 176/264 V_{RMS},
Input power: P_{in} = 2kW,
Output voltage: U_o = 350 V

The design procedure yields the following parameter values: L = 37.6mH, and $C_1 = C_2$ = 127 μF.

The Fig. 4 shows the simulated input current waveform for the two input voltages: U_g=176 V_{RMS} and U_g=230 V_{RMS}. In the latter case, the input current peak value is 16.26 A, the fundamental current amplitude is 13.1 A, the cos(ϕ) is 0.94 and the power factor is 0.91. In order to maintain the same output voltage value, the switch on-time was reduced to 6.1ms (θ_d = 0).

With the chosen output voltage value, at the maximum input voltage the regulation is lost below 3% of the nominal load. Below U_g = 247 V_{RMS}, a complete output voltage regulation from no load to full load is achieved.

For the purpose of comparison, a simple L-C_L filter, at the same output power, complies with the standard with 28mH, peak current value of 20.19 A, cos(ϕ) of 0.695, and power factor of 0.682. The resulting output voltage is 188V at 230 V_{RMS} input voltage.

B) Design for Compliance with Standards.

If the goal is to comply with the standard without care for the output voltage regulation at different input voltage values, the inductance value can be significantly reduced. Considering the previous example, compliance with the standard can be achieved with L = 17.2mH, $C_1 = C_2$ = 45.4 μF, (T_d = 0s, T_{ON} = 4ms, I_{g_pk} = 15.32 A, I_{1_pk} = 12.66 A, cos(ϕ) = 0.973, PF = 0.943). The capability of voltage regulation against load variations is maintained, while it is lost for input voltage variations.

The Fig. 5 shows the line-frequency commutated boost circuit together with the input current waveform. For the purpose of comparison, a line-frequency commutated boost, as used in air conditioning apparatus [7], would need an inductance of 22mH in order to comply with the standard, at U_o = 298.5 V.

a)

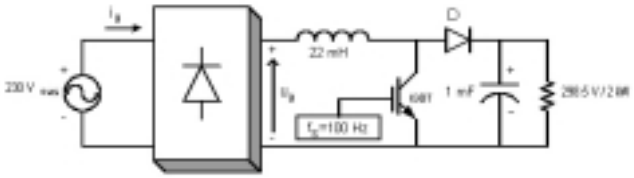

b)

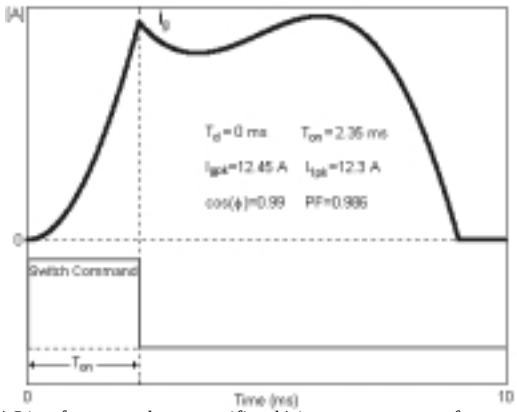

Fig. 5 – a) Line-frequency boost rectifier; b) input current waveform together with switch command signal.

IV. Static Characteristic, PF and Displacement Factor

The static characteristic is given in eq. (8). The Fig. 6 shows the U_o and U_{20} voltage as a function of the angle θ_{on} for two different α values.

Due to boost action, U_o increase with θ_{on} in the range U_{20} is not zero. This range decreases as α increases, also reducing the maximum voltage U_o. For α=1.03, U_{omax}=435V, while for α=2.5 U_{omax}=325V.

$$U_o = \frac{\alpha^2\sqrt{U_{pk}^2 - U_{20}^2}}{\alpha^2 - 1}\left\{\text{sen}(\theta_{on} - \theta_1) - \frac{1}{\alpha}\text{sen}\left[\alpha(\theta_{on} - \theta_1)\right]\right\} + \frac{U_{20}}{\alpha^2 - 1}\left\{\alpha^2\cos(\theta_{on} - \theta_1) - \cos\left[\alpha(\theta_{on} - \theta_1)\right] + \alpha^2 - 1\right\} \quad (8)$$

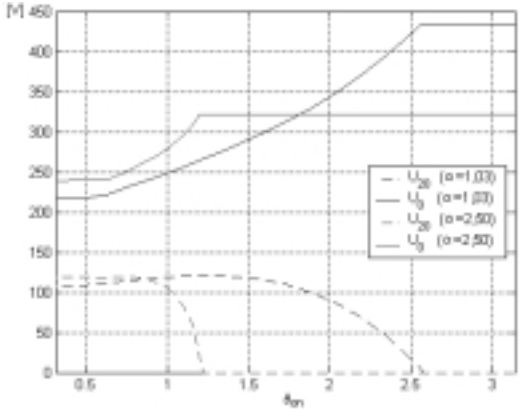

Fig. 6 – Behavior of the U_o and U_{20} voltages as a function of the θ_{on}.

The fig. 7 indicates the behavior of PF and cos(ϕ) as a function of the normalized frequency α and the angle θ_{on}. The depression region in the graphics 7a), for small θ_{on} values, is

due to a severe current distortion that occurs in such situation. PFmax=0.98 for α=1.57 and $\cos(\phi)_{max}$=0.999 for α=1.73.

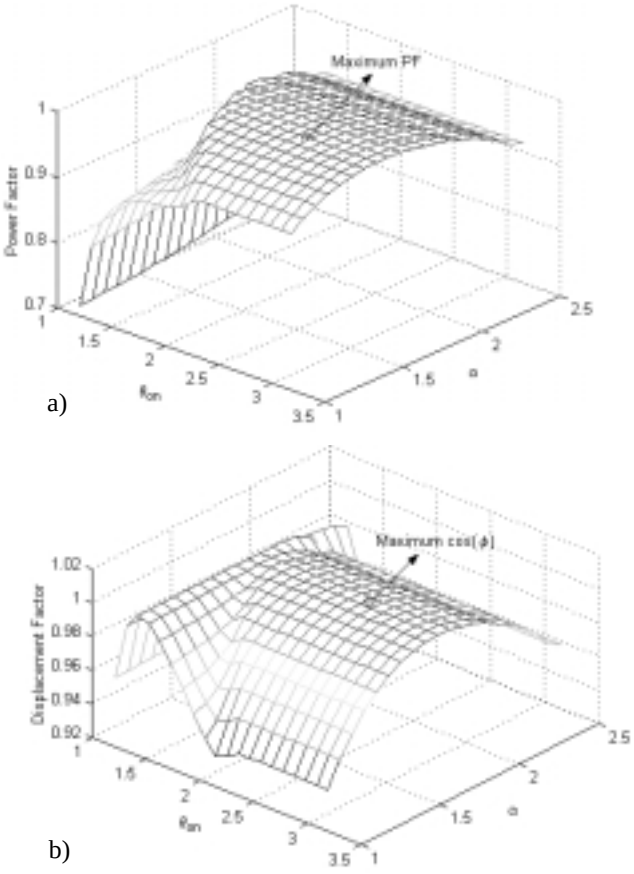

Fig. 7 – Behavior of the PF a) and cos(ϕ) b) in the plane θ_{on} - α. [U_g=220 V_{RMS}, U_o=350 V and L=37.6 mH]

IV. Experimental Results

The Fig. 8 indicates a 2 kW prototype that was built and tested. The following parameters were calculated using the approach for maximum output voltage regulation:

U_g = 176/264 V_{RMS}

L = 31 mH (available at the laboratory)

$C_1 = C_2$ = 126 µF

C_L = 940 µF

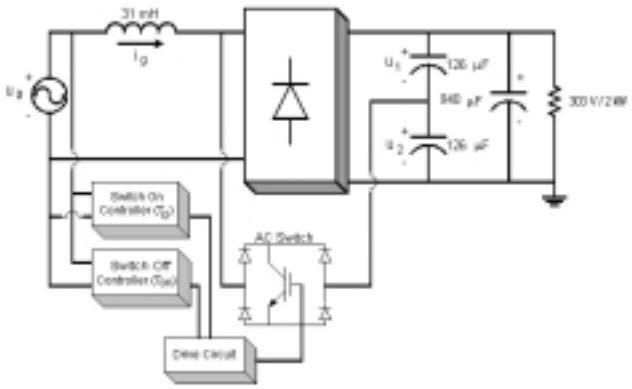

Fig. 8 – Converter circuit.

The resulting waveforms are shown in Fig. 9. The switch command signal is high during all the time for U_g = 176V_{RMS}. The current through the auxiliary switch stops when the auxiliary capacitor current zeroes. The resulting power factor is 0.97. The output voltage is regulated in 303V, lower than expected due to converter losses. The measured efficiency is 91%.

For U_g = 220V_{RMS} the auxiliary switch changes the duty-cycle, altering the input current shape but maintaining the output voltage constant. For this situation the input voltage and current waveforms are shown in Fig. 10. The measured efficiency has increased to 93 % due to the lower current value. The power factor is 0.95. The current spectrum is shown in Fig. 11 together with class A limits.

For the maximum input voltage, the input voltage and current waveforms are shown in Fig. 12. The output Voltage is 302 V, the efficiency is 95 % and the power factor is 0.93.

Without the auxiliary circuit operation, the resulting waveforms are shown in Fig. 13 for the rated voltage. The output voltage drops to 211 V, thus reducing the output power to 844 W. The efficiency is 93% and the Power Factor is 78%.

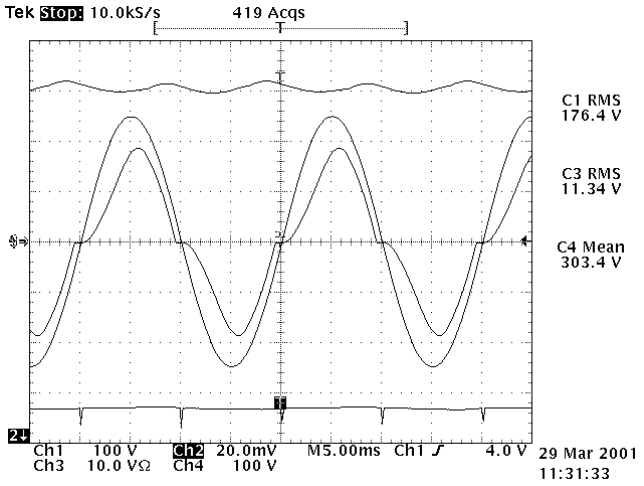

Fig. 9 – Waveforms at minimum input voltage (176V_{RMS}): Output voltage (100 V/div); Line voltage (100V/div); Line current (10 A/div) and switch command.

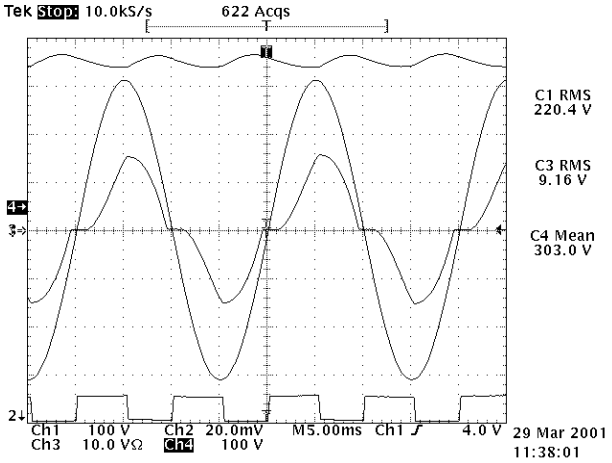

Fig. 10 – Waveforms at nominal input voltage (220V_{RMS}): Output voltage (100 V/div); Line voltage (100V/div) and current (10 A/div) and switch command.

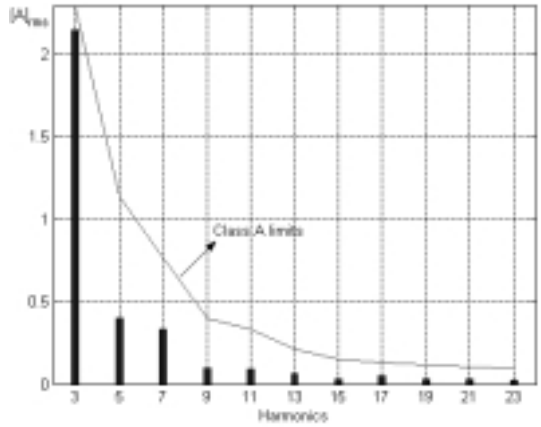

Fig. 11 – Input current spectrum at 220 V_{RMS}.

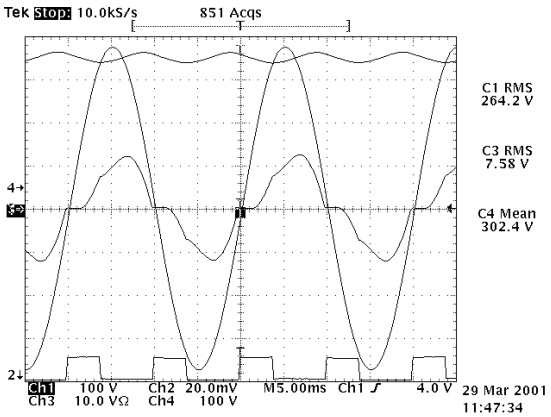

Fig. 12 – Waveforms at maximum input voltage (264V_{RMS}): Output voltage (100 V/div); Line voltage (100V/div) and current (10 A/div) and switch command.

For all the situations the output voltage is lower than the expected due to the non unity converter efficiency.

Comparing the results with and without the auxiliary circuit, it is clear that, without additional losses, it is possible to reduce the current distortion, thus improving the power factor, and to stabilize the output DC voltage in a wide input voltage variation range.

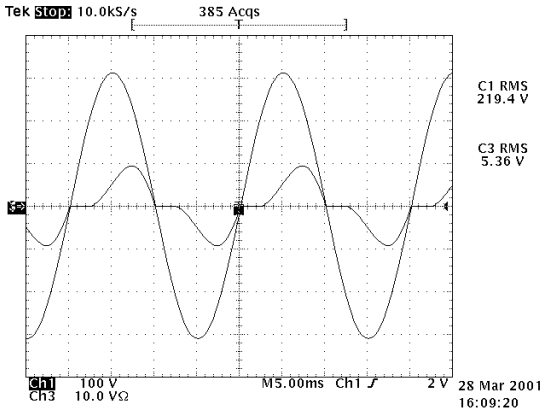

Fig. 13 – Waveforms with passive filter, at rated input voltage (220V_{RMS}): Line voltage (100V/div) and current (10 A/div).

V. Conclusions

The presented add-on line-frequency commutated cell is able to greatly improve both power factor and output voltage regulation of rectifiers with passive L-C filters. The boost action allows for the compensation of the voltage drop across the input filter inductor, so as output voltages higher than the peak of the line voltage can be achieved.

Moreover, as compared to the line-frequency commutated boost rectifier, the proposed circuit allows compliance with the low-frequency harmonic standard IEC 61000-3-2 with a lower filter inductance value, at output power levels greater than 1kW.

A converter prototype was built and tested, verifying the expectations.

VI. Acknowledgment

The authors wish to acknowledge the support of FAPESP (Fundação de Amparo à Pesquisa do Estado de São Paulo).

VII. References

1. IEC 1000-3-2, First Edition 1995-03, Commission Electrotechnique Internationale, 3, rue de Varembé, Genève, Switzerland.
2. M. Jovanovic, D. E. Crow, "Merits and Limitations of Full-Bridge Rectifier with LC Filter in Meeting IEC 1000-3-2 Harmonic-Limit Specifications," IEEE Applied Power Electronics Conf. Proc. (APEC), March 1996, pp. 354-360.
3. I. Suga, M. Kimata, Y. Ohnishi, R. Uchida, “New Switching Method for Single-Phase AC to DC Converter”, PCC Conf. Proc., Yokohama, 1993, pp. 93-98
4. L. Rossetto, G. Spiazzi, P. Tenti, "Boost PFC with 100Hz Switching Frequency providing Output Voltage Stabilization and Compliance with EMC Standards," IEEE Transaction on Industry Applications, vol.36, n.1, January/February, 2000, pp.188-193.
5. S. Buso, G. Spiazzi, “A Line-Frequency Commutated Rectifier Complying with Standards”, IEEE Applied Power Electronics Conf. Proc. (APEC), March, 1999, pp. 356-362.
6. J. A. Pomilio, G. Spiazzi, “A Double-Line-Frequency Commutated Rectifier Complying with IEC 1000-3-2 Standards”, IEEE Applied Power Electronics Conf. Proc. (APEC), March, 1999, pp. 349-355.
7. Y. Shimma, K. Iida, “Inverter Applications to Air Conditioning Field”. International Power Electronics Conf. - IPEC, Japan, 2000, pp. 1747-1750.